 FDMP, vol.5, no.4, pp.411-424, 2009

On the Application of Wavelets to One Dimensional Flame Simulations with Non-Unit Lewis Numbers

R. Prosser[1]

Abstract: A novel wavelet-based method for the simulation of reacting flows on adaptive meshes is presented. The method is based on a subtraction algorithm, wherein the wavelet coefficients are calculated from the low resolution up (as opposed to the standard top-down approach). The advantage of this new method is that it allows the calculation of wavelet coefficients on sparse grids, and thus lends itself more readily to adaptive computational meshes than does the traditional wavelet algorithm. The approach is used to simulate a one-dimensional laminar pre-mixed flame with different Lewis numbers. The computational grid is adapted via the removal of grid points whose wavelet coefficients are small with reference to some user-specified threshold. To circumvent the difficulties associated with the strongly nonlinear reaction rate terms, the scheme simulates flow behaviour in the physical (i.e. not transformed) domain, and the wavelets thus provide the method by which the derivatives appearing in the transport equations are calculated. A number of simulations are presented which demonstrate the efficiency of the method.

Keywords: Wavelets, partial differential equations, turbulent combustion

1 Introduction

For most flows of industrial relevance, there typically exists a wide spectrum of length and time scales in the evolving physical processes. This is particularly true of premixed combustion, where the flame structure can typically occupy $O(1)mm$, while the burner geometry in which it sits can be tens or even hundreds of times larger. This scale separation presents a challenge to traditional numerical methods, but is well suited to discretizations based on wavelets. Wavelets characterize a function in terms of its (appropriately defined) gradients [Daubechies (1992)]; as such, they automatically track regions of rapid change in the flow structure, such as

[1] Department of MACE, University of Manchester, Manchester M60 1QD

might be found in a flame. Wavelets thus provide an elegant framework in which to develop an adaptive meshing strategy.

The use of wavelets as a tool for the numerical simulation of fluid flow can be traced back to Liandrat and Tchamitchian [Liandrat and Tchamitchian (ICASE Report, December 1990)], and to Bacry, Mallat and Papanicolou [Bacry, Mallat, and Papanicolaou (1992)]. These authors used orthogonal wavelets and developed schemes that could exploit the asynchronous evolution of the solution in time and space. This line of development can be seen in recent methods proposed by—for example—Domingues et al [Domingues, Gomes, Roussel, and Schneider (2008)]. The approach has led to methods both for non reactive flows (such as those found in the works of Vasilyev et al [Vasilyev, Paolucci, and Sen (1995); Vasilyev and Paolucci (1997)], and others [Bacry, Mallat, and Papanicolaou (1992); Fröhlich and Schneider (1995)]) and for reactive flows (i.e. Fröhlich et al. [Fröhlich and Schneider (1997, 1996)], Singh et al [Singh, Rastigejev, Paolucci, and Powers (2001)], Prosser [Prosser (1997)] and more recently, the work of Roussel et al [Roussel and Schneider (2006b,a)]). Many of the early methods developed were applicable only to periodic domains, which presents a problem to combustion simulations—the reactants flowing into a domain have significantly different properties to the products flowing out. Wavelets defined on non-periodic intervals are much more difficult to construct using the classical (i.e. Fourier based) methods of derivation, and it is here that the so-called *second generation approach* developed predominantly by Sweldens et al [Sweldens (1996, 1997); Schröder and Sweldens (2000)] makes a major contribution. In the second generation approach, there is no need for a projection quadrature and the dependent variables themselves can be used directly as the scaling function coefficients. Fast wavelet transforms exist for the evaluation of the wavelet coefficients, and constructions for bounded intervals are straightforward to implement. The original contribution made by this paper lies in the development of an alternative strategy for the calculation of second generation wavelet coefficients—we have termed it a *subtraction strategy*. We use biorthogonal interpolating wavelets proposed by Donoho [Donoho (1992)] with $N = 4$ (i.e. the scaling functions span up to cubic polynomials), and which can be shown to be fourth order accurate [Prosser (2007a)]. The approach will work with interpolating wavelets of any order, and thus even higher order accuracy adaptive methods can be obtained if required.

In the following paper, section 2 briefly reviews the technical aspects of the subtraction strategy. The laminar flame problem is described in section 3, and section 4 provides the results obtained using the discretization method. Section 5 ends the paper with a discussion of some of the problems facing the existing discretization method.

2 Subtraction strategy

For reacting flow systems, solving the governing equations in the physical domain (as opposed to the transform domain) is more appealing, as the reaction rates can be calculated directly; wavelet methods are then used purely to calculate the derivatives appearing in the transport equations [Singh, Rastigejev, Paolucci, and Powers (2001)]. The sparsity of the wavelet representation provides a particularly elegant framework for adaptive calculations, but the main difficulty in this approach lies in calculating the wavelet coefficients in the first place. Each pass of a standard wavelet transform is akin to a finite difference operation, and works from the finest resolution down to the coarsest [Daubechies (1992)]. Consequently, in discretizing a dependent variable adaptively using a traditional approach, we are faced with the *hanging node problem* (i.e. internal nodes in the discretisation may not have all the neighbour points required to derive their wavelet coefficients). To circumvent this problem, we have developed a *subtraction based wavelet transform* [Prosser (2007a)]. Using the traditional nomenclature of wavelet methods [Cohen, Daubechies, and Feauveau (1992)], the projection of some function f onto a scaling function space $\mathbf{V}_i$ is denoted as$P_i(f)$. The corresponding projection onto a wavelet space $\mathbf{W}_i$ is denoted $Q_i(f)$. The subtraction transform can then be written as [Prosser (2007a)]

$$Q_{J-m}(f(x)) = P_{J-m+1}[P_J - P_{J-m}](f(x)), \tag{1}$$

for the coarsest resolution, and

$$Q_{J-m+1}(f(x)) = P_{J-m+2}((P_J - P_{J-m}) - Q_{J-m})(f(x)) \tag{2}$$

for the next resolution; a similar expression exists for each successive resolution, and $J-m<J$ specifies a minimal coarse resolution for the discretisation. We note that this approach also differs from standard wavelet transforms in that we keep a low resolution scaling function space (denoted $\mathbf{V}_{J-m}$). The coefficients belonging to $\mathbf{V}_{J-m}$ will *always* be retained, regardless of adaption strategy. Their regular structure forms the foundations on top of which the adaptive points are added. The wavelet coefficients are denoted by $d_{i,k}$ for $J-m \leq i \leq J-1$, and $0 \leq k \leq 2^i-1$. An adaptive grid will emerge during the computation only if those points associated with 'large' wavelet coefficients are retained. In practice, we retain $d_{i,k}$ (and its associated grid point) if $|d_{i,k}| > \varepsilon$, where ε is some user specified threshold.

The advantage of using equations 1, 2 and their successors lies in the fact that by construction, the hanging nodes in the original adaptive discretization are surrounded by zeros in the representation of $(P_J - P_{J-m})(f)$; consequently, storage of the surrounding nodes is no longer required [Prosser (2007a)]. Each pass of the

subtraction step maps features of a given length scale (denoted by $J-m$, $J-m+1,\ldots,J-1$) to zero, and the wavelet coefficients are the remainder from this subtraction at the next finest length scale. This approach has a more involved structure than the traditional method, but its principal advantage is that the forward transform can be obtained regardless of the fine scale grid structure: we do not require a full, structured grid to calculate the wavelet coefficients. If, during the calculation of a particular wavelet coefficient, a neighbouring point does not exist, then this implies that the neighbour's wavelet coefficient is less than the specified threshold. Consequently, the contribution of the neighbouring point—had it existed—would have been mapped essentially to zero (i.e. to within ε) by the action of the preceding subtraction steps. The practical implementation of this algorithm is quite involved, and we refer to [Prosser (2007a)] for a fuller description.

3 Implementation

3.1 Problem background

The equations governing a gaseous reacting system consisting of N_s species may be written as [Williams (1985)]

$$\begin{aligned}
\frac{\partial \rho}{\partial t}+\frac{\partial}{\partial x}(\rho u) &= 0\\
\frac{\partial \rho u}{\partial t}+\frac{\partial}{\partial x}(\rho uu+p) &= \frac{\partial}{\partial x}(\tau_{xx})\\
\frac{\partial \rho E}{\partial t}+\frac{\partial}{\partial x}(u(\rho E+p)) &= -\frac{\partial q}{\partial x}+\frac{\partial}{\partial x}(u\tau_{xx})\\
\frac{\partial \rho Y_l}{\partial t}+\frac{\partial}{\partial x}(\rho uY_l) &= \omega_l+\frac{\partial}{\partial x}\left(\rho D\frac{\partial Y_l}{\partial x}\right) \qquad l=1,2,\ldots,N_s.
\end{aligned} \tag{3}$$

This coupled set of partial differential equations is not limited to low Mach number flows and consequently, acoustic phenomena—particularly those arising from initial condition transients—will be resolved. We choose to retain the full complexity of the compressible flow equations because these reflect our interest in thermoacoustic instabilities.

In equation 3(b) and (c), τ_{xx} is the viscous stress. The heat flux vector q is defined as

$$q=-\lambda\frac{\partial T}{\partial x}+\sum_{l=1}^{N_s}h_l\rho D\frac{\partial Y_l}{\partial x}. \tag{4}$$

The thermal conductivity is given by a modified form of the equation proposed by

Echekki et al [Echekki and Chen (1996)]:

$$\lambda = \lambda_0 c_p \left(\frac{T}{T_0} \right),$$

where $\lambda_0 = 2.58 \times 10^{-5} kg/(ms)$. The temperature dependence of the conductivity is set such that an analytic benchmark solution can be derived via asymptotic methods [Williams (1985); Bush and Fendell (1970)]. The benchmark solution will be used later in the paper. The viscosity and mass diffusivity appearing in the transport equations are derived via the assumptions of constant Prandtl number and constant Lewis number, where

$$\mathrm{Pr} = \frac{\mu c_p}{\lambda}, \quad Le = \frac{\lambda}{\rho D c_p}.$$

For this study, the Prandtl number is assumed to be given by $\mathrm{Pr} = 0.75$, the specific heats and the molecular weights of the components are assumed to be constant, with $c_p = 1005 J/kgK$, $\gamma = 1.4$ and $W = 28.96 kg/kmol$.

The stagnation internal energy is obtained using

$$E = e_{N_s} + \sum_{l=1}^{N_s - 1} (e_l - e_{N_s}) Y_l + \frac{u^2}{2}, \tag{5}$$

where e_l is the species internal energy, comprising the internal energy of formation e_l^0, and a sensible component:

$$e_l = e_l^0 + \int_{T_0}^{T} c_v \left(T' \right) dT'.$$

Equation 5 has been written such that the constraint

$$\sum_{l=1}^{N_s} Y_l = 1$$

is automatically satisfied, and where Y_{N_s} is usually treated in combustion problems as the mass fraction of the diluent (typically nitrogen for reacting hydrocarbon-air simulations). The pressure is calculated from the thermal equation of state

$$p = \rho R_l T \sum_{l=1}^{N_s - 1} (R_l - R_{N_s}) Y_l, \tag{6}$$

where R_l is the characteristic gas constant for species Y_l.

For the single step chemical reaction mechanism considered here

Reactants → Products,

$N_s = 2$ and the thermochemical state of the gas is characterized by a *progress variable.* The progress variable takes a value of 0 in the reactants and 1 in the products. For consistency with other combustion studies, we define the progress variable as $c \equiv Y_1$ in our simulations, and the reaction rate is assumed as [Williams (1985)]

$$\omega = \rho B^* (1-c) \exp\left(\frac{-\beta\left(1-\widehat{T}\right)}{1-\alpha\left(1-\widehat{T}\right)}\right). \tag{7}$$

with $\omega_1 = -\omega_2$. B^* is the frequency factor ($= 285.1 \times 10^{-3} s^{-1}$ in this study), $\beta (= 6)$ is the Zeldovich number, $\widehat{T}$ is the reduced temperature;

$$\widehat{T} = \frac{T - T_0}{T_{ad} - T_0}$$

with T_0 and T_{ad} being the unburned reactant and adiabatic product temperature, respectively. α is related to the heat release of the fuel, and is set to 0.8 here. This corresponds to an adiabatic flame temperature of $1500K$ for an inlet temperature of $300K$.

We define the laminar flame speed as the rate at which an unperturbed flame propagates into a quiescent reactant. To derive an expression for this quantity, we re-examine equation 3(d) in the light of a unidimensional, single step reaction problem;

$$\frac{\partial \rho c}{\partial t} + \frac{\partial}{\partial x}(\rho u c) = \omega + \frac{\partial}{\partial x}\left(\rho D \frac{\partial c}{\partial x}\right). \tag{8}$$

We assume a domain whose length is sufficient to encompass the flame structure entirely, and integrate equation 8 over this domain to obtain

$$\int \frac{\partial \rho c}{\partial t} dx + \rho u c|_L^R = \int \omega dx + \left(\rho D \frac{\partial c}{\partial x}\right)\Big|_L^R. \tag{9}$$

where L and R are the left and right hand ends of the domain, respectively. The boundary conditions for the progress variable are

$$\begin{aligned} c_l &\simeq 0 \simeq \left(\rho D \frac{\partial c}{\partial x}\right)\Big|_L \\ c_R &= 1 \\ \left(\rho D \frac{\partial c}{\partial x}\right)\Big|_R &= 0 \end{aligned}$$

The approximate values for the left hand of the domain arise from the cold boundary problem—the chemical reaction term is non-zero even in reactants at ambient temperature [Bush and Fendell (1970)]. These approximate conditions notwithstanding, the boundary conditions on the progress variable allow equation 9 to be written as

$$\int \frac{\partial \rho c}{\partial t} dx + \rho u = \int \omega dx$$

Now, we set $u = s_l^0$, the laminar flame speed , with

$$s_l^0 = \rho^{-1} \int \omega dx,$$

thereby ensuring that

$$\int \frac{\partial \rho c}{\partial t} dx = 0.$$

By setting the inlet velocity for our simulations equal to the laminar flame speed, a stationary flame profile is obtained. This specification gives a simulation Mach number of $O\left(10^{-3}\right)$ based on the laminar flame speed.

3.2 Simulation code details

A wavelet based code has been developed at the University of Manchester for the simulation of compressible laminar flames. The code solves the transport equations given in the previous section, and can apply the subtraction algorithm to the flow field via any family of basis functions. $N = 4$ interpolating wavelets have been used here and separate convergence tests have confirmed that the scheme has 4^{th} order accuracy when applied to a regular (full) discretization [Prosser (2007b)]. The governing equations are integrated in time using the minimal storage fourth order Runge-Kutta method proposed by Wray [Wray (1990)]. The maximum resolution allowed in the simulation was set at 512 grid points. The simulation set-up is completed via the specification of non-reflecting (time-dependent) boundary conditions [Poinsot and Lele (1992); Prosser (2005)]

4 Results

Figure 1 depicts the laminar flame profiles for pressure, density, velocity and reaction rate based on a unit Lewis number flame. An asymptotic solution of Williams [Williams (1985)]—based on high activation energies—has been used to provide a benchmark for assessing the accuracy of the approach. A previous study for the case of unit Lewis number has found excellent agreement between the numerical

and analytically predicted profiles, with a maximum error of around 5% [Prosser (2007a)]. The disparity between the two appears to be due to the comparatively low Zeldovitch number ($\beta = 6$) used in the asymptotic analysis.

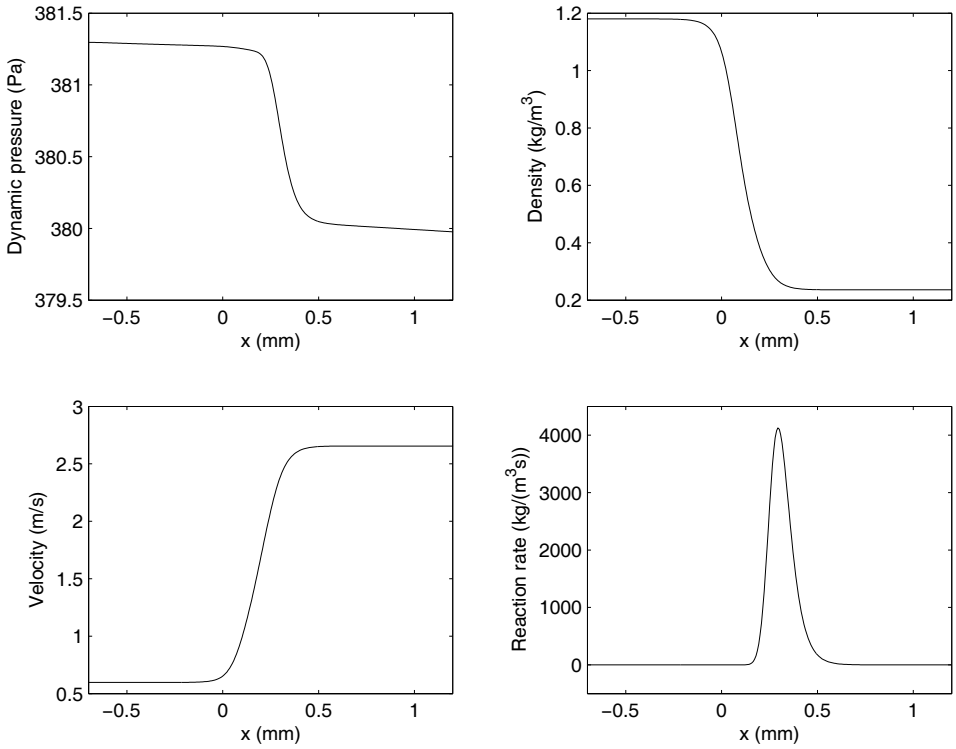

Figure 1: Benchmark solution for unit Lewis number flame

A global measure of the scheme's accuracy is provided by a comparison with asymptotic estimates for the laminar flame speed eigenvalue [Williams (1985)]. Expressions for this quantity have been derived by Bush and Fendell [Bush and Fendell (1970)], and have served as the principal performance measure for the computational studies reported by Peters and Warnatz [Peters and Warnatz (1982)]. For the planar flame configuration studied here, the second order estimate of the flame speed is given by [Peters and Warnatz (1982)]

$$\frac{\rho B^* \lambda}{m^2 c_p} = \frac{\beta^2}{2Le}\left(1 + \frac{2}{\beta}(2\alpha - 2.344 + Le) + O\left(\beta^{-2}\right)\right), \tag{10}$$

where $m = \rho^0 s_l^0$ and all other quantities are evaluated in the reactant stream. For the wavelet scheme with $\varepsilon = 0$, table 1 provides the numerically evaluated laminar

flame speeds for the three different Lewis numbers. In each case the agreement is excellent, with errors in the flame speed estimates no greater than about 2%.

Having established the parity between the $\varepsilon = 0$ (full) solution and the asymptotic solution, we use the former as the benchmark —additional results for non-unit Lewis number flames can be more easily obtained than via the asymptotic analysis.

Figure 2 shows the reaction rate profiles obtained for the three flames with $\varepsilon = 10^{-6}$. The reaction rates exhibit a systematic trend toward lower flame speeds as the Lewis number decrease; Using the $Le = 1$ case as baseline, the $Le = 0.9$ case provides a flame with a 3.3% decrease in flame speed, while the $Le = 1.1$ flame has a 3.6% higher flame speed. This result is consistent with equation 10.

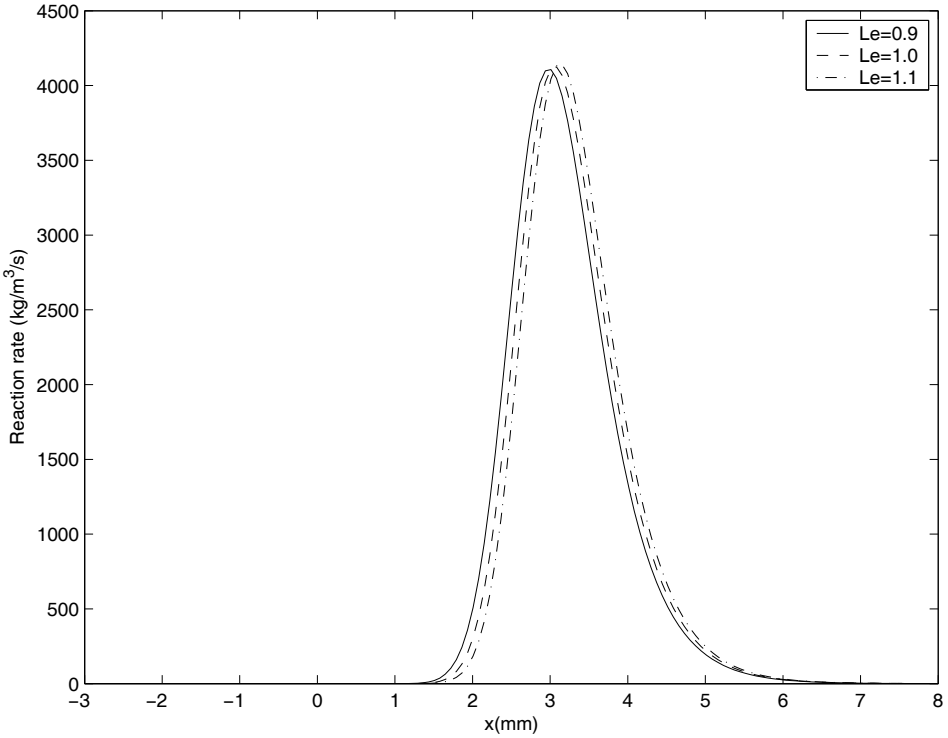

Figure 2: Reaction rates for flames with different Lewis numbers

Table 2 shows the dependence of the laminar flame speeds with threshold. The dependence of the flame speed with wavelet threshold is found to be very weak. Using two threshold levels separated by two orders of magnitude ($\varepsilon = 10^{-4}$ and $\varepsilon = 10^{-6}$), we found that the change in flame speed was of the order of 0.1%. The

Table 1: Comparison of laminar flame speed eigenvalues for different Lewis numbers

Le	$\left(s_l^0\right)_{asy}(m/s)$	$\left(s_l^0\right)_{num}(m/s)$
0.9	0.486	0.4997
1.0	0.506	0.5166
1.1	0.524	0.5354

Table 2: Sensitivity of flame speed to choice of threshold. Δs_l^0 is evaluated as the difference in the flame speeds obtained with $\varepsilon = 10^{-6}$ and $\varepsilon = 10^{-4}$

Le	$s_l^0(m/s)$	$\left\|\Delta s_l^0\right\|(\%)$
0.9	0.486	0.0747
1.0	0.506	0.1161
1.1	0.524	0.0600

reason for this lies in the fact that the wavelet coefficients are at their largest in the region of sharpest curvature—these regions are themselves strongly correlated with the reaction rate [Williams (1985)]. Consequently, thresholding acts preferentially in areas furthest from the reaction zone, and migrates toward the flame structure itself only as the threshold becomes significant.

Figure 3 shows part of the flame structure defined on the adapted component of the grid for $\varepsilon = 10^{-4}$ and unit Lewis number. Similar results have been obtained for the other Lewis numbers under study. The number of retained grid points for this simulation was typically 136; this represents a reduction of 73% over the original full discretisation of 513 grid points. The figure clearly shows how the wavelets have 'attached' themselves to the regions of the flow where the curvature is largest. Here, the solution was adapted to the density and momentum equations; if we were to adapt on the reaction rate, then we would expect a clustering of nodes in and around the regions of maximum reaction rate; this would yield a different points distribution. It is as yet unclear which family of dependent variables forms an optimal set on which to threshold; this remains as ongoing work.

5 Conclusions and future work

In this paper, we have applied interpolating biorthogonal wavelets to laminar premixed flames with Lewis numbers of 0.9, 1 and 1.1. The wavelet coefficients are calculated by a novel subtraction based strategy that requires only a very coarse regular grid. Results for a non-zero wavelet threshold show that the wavelet coefficients cluster around the reaction zone in the flame; the quality of the solution is

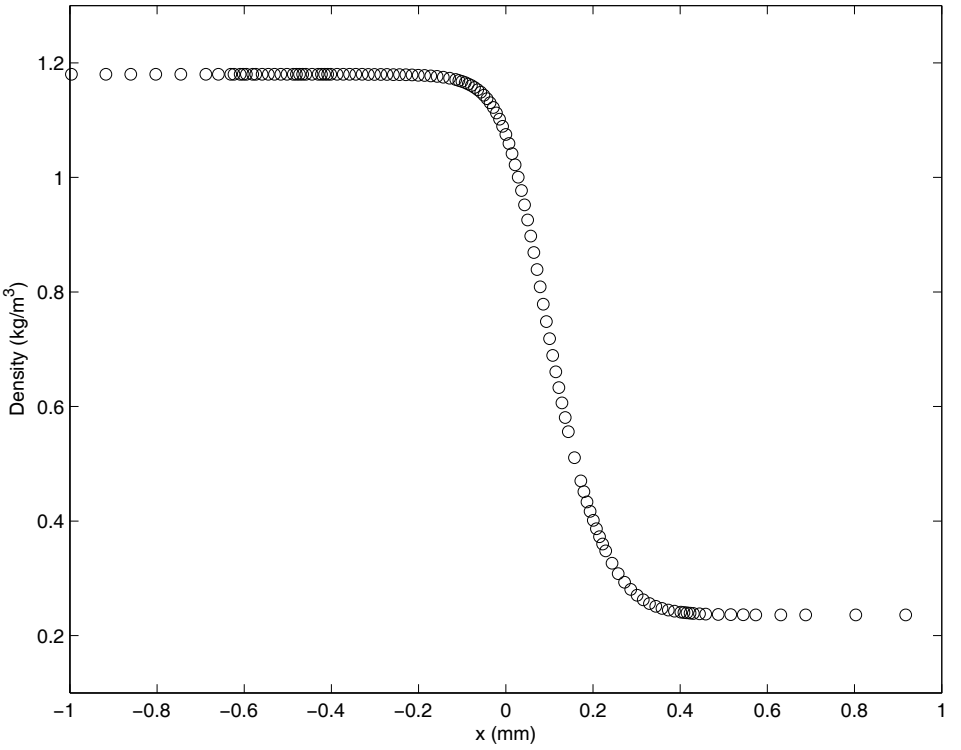

Figure 3: Density profile for unit Lewis number flame, showing adaptive grid points for threshold set at $\varepsilon = 10^{-4}$

excellent—this is despite the fact that the adapted mesh contains only $\sim 25\%$ of the elements in the original full discretization.

The principal future development of this method lies in the reworking of the current transform algorithm to make it yet faster; this is particularly important in two and three dimensional discretizations, where the initial subtraction steps embedded in terms like $\left(P_J^{(2)} - P_{J-m}^{(2)}\right) f$ (two-dimensional) and $\left(P_J^{(3)} - P_{J-m}^{(3)}\right) f$ (three dimensional) are currently comparatively expensive to evaluate. Also, for reacting flow systems with multiple coupled variables, the systematic selection of an appropriate threshold—and its subsequent effects on the hydrodynamic field or reaction chemistry—is as yet unclear. In a future work, we will seek to develop a more systematic method of selecting thresholds that are appropriate for coupled variables that may differ by many orders of magnitude.

Acknowledgement: The author is grateful for the helpful and constructive com-

ments made by the referees on the early drafts of this paper.

References

Bacry, E.; Mallat, S.; Papanicolaou, G. (1992): A Wavelet Based Space-Time Adaptive Numerical Method for Partial Differential Equations. *Math. Modelling and Num. Anal.*, vol. 26, no. 7, pp. 793–834.

Bush, W.; Fendell, F. E. (1970): Asymptotic Analysis of Laminar Flame Propagation for General Lewis Numbers. *Comb. Sci. Tech.*, vol. 1, pp. 421–428.

Cohen, A.; Daubechies, I.; Feauveau, J. (1992): Biorthogonal Bases of Compactly Supported Wavelets. *Commun. Pure Appl. Math.*, vol. 45, pp. 485–560.

Daubechies, I. (1992): *Ten lectures on wavelets*. SIAM, Philadelphia. CBMS Lecture notes, No. 61.

Domingues, M.; Gomes, S.; Roussel, O.; Schneider, K. (2008): An adaptive multiresolution scheme with local time stepping for evolutionary PDEs. *J. Comp. Phys.*, vol. 227, pp. 3758–3780.

Donoho, D. (1992): Interpolating Wavelet Transforms. Presented at The NATO Advanced Study Institute conference on 'Wavelets and Applications', Il Ciocco, Italy, 1992.

Echekki, T.; Chen, J. (1996): Unsteady Strain Rate and Curvature Effects in Turbulent Premixed Methane-Air Flames. *Combustion and Flame*, vol. 106, pp. 184–202.

Fröhlich, J.; Schneider, K. (1995): Numerical Simulation of Decaying Turbulence in an Adapted Wavelet Basis. *Appl. Comput. Harm. Anal.*, vol. 2, pp. 393–397.

Fröhlich, J.; Schneider, K. (1996): A Fast Algorithm for Lacunary Wavelet Bases related to the Solution of PDEs. *C. R. Math. Rep. Acad. Sci. Canada*, vol. XVI, pp. 83–86.

Fröhlich, J.; Schneider, K. (1997): An Adaptive Wavelet-Vaguelette Algorithm for the Solution of PDEs. *J. Comp. Phys.*, vol. 130, no. 174-190.

Liandrat, J.; Tchamitchian, P. (ICASE Report, December 1990): Resolution of the 1-D Regularised Burgers Equation using a Spatial Wavelet Approximation. Technical Report 90-83, NASA, ICASE Report, December 1990.

Peters, N.; Warnatz, J.(Eds): *Numerical Methods in Laminar Flame Propagation*. Notes on Numerical Fluid Mechanics. Vieweg.

Poinsot, T.; Lele, S. (1992): Boundary Conditions for Direct Simulations of Compressible Viscous Flows. *J. Comp. Phys*, vol. 101, pp. 104–129.

Prosser, R. (1997): *Numerical Methods for the Computation of Combustion*. PhD thesis, Cambridge University, 1997.

Prosser, R. (2005): Improved Boundary Conditions for the Direct Numerical Simulation of Turbulent Subsonic Flows I: Inviscid Flows. *J. Comp. Phys.*, vol. 207, pp. 736–768.

Prosser, R. (2007): An Adaptive Algorithm For Compressible Reacting Flows Using Interpolating Wavelets. *Proc. Instn. Mech. Engrs., Part C*, pp. 1397–1410.

Prosser, R. (2007): On the Effects of Lifted Wavelets for Combustion Simulations. *Proc. Instn. Mech. Engrs., Part C*, pp. 1579–1596.

Roussel, O.; Schneider, K. (2006): Adaptive numerical simulation of pulsating flames for large Lewis and Zeldovich ranges. *Comm. Nonlin. Sci. Num. Sim.*, vol. 11, pp. 463–480.

Roussel, O.; Schneider, K. (2006): Numerical study of thermodiffusive flame structures interacting with adiabatic walls using an adaptive multiresolution scheme. *Combust. Theory Modelling*, vol. 10, pp. 273–288.

Schröder, P.; Sweldens, W. (2000): *Building Your Own Wavelets at Home*. Lecture Notes in Earth Sciences Vol. 90. Springer.

Singh, S.; Rastigejev, Y.; Paolucci, S.; Powers, J. (2001): Viscous detonation in $H_2 - O_2 - Ar$ using intrinsic low-dimensional manifolds and wavelet adaptive multilevel representation. *Combust. Theory Modelling*, vol. 5, pp. 163–184.

Sweldens, W. (1996): The Lifting Scheme: A Custom Design Construction of Biorthogonal Wavelets. *Appl. Comput. Harm. Anal.*, vol. 3, pp. 186–200.

Sweldens, W. (1997): The Lifting Scheme: A Construction of Second Generation Wavelets. *SIAM J. Math. Anal.*, vol. 29, pp. 511–546.

Vasilyev, O.; Paolucci, S.; Sen, M. (1995): A Multilevel Wavelet Collocation Method for Solving Partial Differential Equations in a Finite Domain. *J. Comp. Phys.*, vol. 120, pp. 33–47.

Vasilyev, O. V.; Paolucci, S. (1997): A Fast Adaptive Wavelet Collocation Algorithm for Multidimensional PDEs. *J. Comp. Phys*, vol. 138, pp. 16–56.

Williams, F. (1985): *Combustion Theory - Second Edition*. Addison Wesley, Menlo Park, California.

Wray, A. (1990): Minimal Storage Time-Advancement Schemes for Spectral Methods. NASA Ames Research Center, 1990.